ARMA 12-222

Analysis of the Influence of Low Conductivity Formations on Slope Stability of Open-Pit Iron Ore Mines

Ventura, L. C.
Geoestável Consultoria e Projetos, Belo Horizonte, MG, Brazil
Bacellar, L. A. P.
University Federal of Ouro Preto, Ouro Preto, MG, Brazil

This paper was prepared for presentation at the 46th US Rock Mechanics / Geomechanics Symposium held in Chicago, IL, USA, 24-27 June 2012.

.

ABSTRACT: This article presents the analysis of the possible influences of low-conductivity phyllites of the Batatal Formation on the flow pattern and on the slope stability of the bottom pit of the Tamandua, Pico and Capitao do Mato iron-ore mines, in the Quadrilátero Ferrífero region, in southeastern Brazil. Typical cross-sections of these mines were selected after a careful analysis of geological, hydrogeological and geotechnical data. The patterns of flow were simulated with SEEP/W® software assuming some boundary conditions and recharge rates provided by adapted characteristic curves for each outcropping units. Limit equilibrium stability analyses were performed with SLOPE/W®, with Bishop, Janbu and Morgenstern/Price methods. From the parametric analysis it can be concluded that: it is better to use unsaturated conductivity curves indirectly determined than to adopt evenly distributed recharge rates through all the geological units; slope stability analyses coupled with flow analyses showed to be very effective; vertical components of flow are important to establish the slope safety factor and can determine local failures; for this reason, high conductivity layers in Batatal Formation, such as metacherts, increase the stability factor; permeability values obtained through back analyses in previous studies suggest that there is a reasonable flow through the Batatal formation rock masses.

1. INTRODUCTION

The lithotypes of low hydraulic conductivity are considered elements that control slope stability because they may behave as geological hydraulic barriers that quite often favor the development of flows with strong vertical components and high hydraulic gradients (Patton & Hendron, 1974; Freeze & Cherry, 1979), which may lead to localized and rock mass failures.

The consequences of these hydraulic barriers, which may be characterized by different dimensions, spatial orientations and geometries, have not been further investigated for quantification purposes. Thus, this work seeks to contribute towards the understanding of the potential influence of phyllites from the Batatal Formation while acting as hydraulic barriers, both on the water flow pattern and on slope stability of open pits in the Quadrilátero Ferrífero (QF) region, State of Minas Gerais, southeastern Brazil.

Those influences can be assessed from the study on the geotechnical conditions of slopes of the Pico, Tamanduá and Capitão do Mato iron ore mines (Figure 1) owned by VALE by means of slope stability analyses in conjunction with the results of the groundwater flow modeling, which was considered effective for each section analyzed through some limit equilibrium methods: Simplified Bishop's Method (1955), Simplified Janbu's Method (1968) and Morgenstern Price's Method (1965); the target has been reached as described at the end of this paper.

2. DESCRIPTION OF AREAS

The Pico, Tamanduá and Capitão do Mato iron ore pits are located on the eastern limb of the Moeda Syncline (Dorr, 1969), southeast of Belo Horizonte (Figure 1), the State capital.

The QF area is approximately 7,190 km^2, and it is partially inserted into the extreme southeast edge of the São Francisco Craton and into the Araçuaí belt, of Brasiliano age (Alkmin & Marshak, 1998). The QF stratigraphy consists of Archaean granitic-gneissic basement complexes, Archaean volcano-sedimentary sequence (Rio das Velhas Supergroup), Proterozoic metasedimentary sequence (Minas Supergroup) and young sedimentary covers.

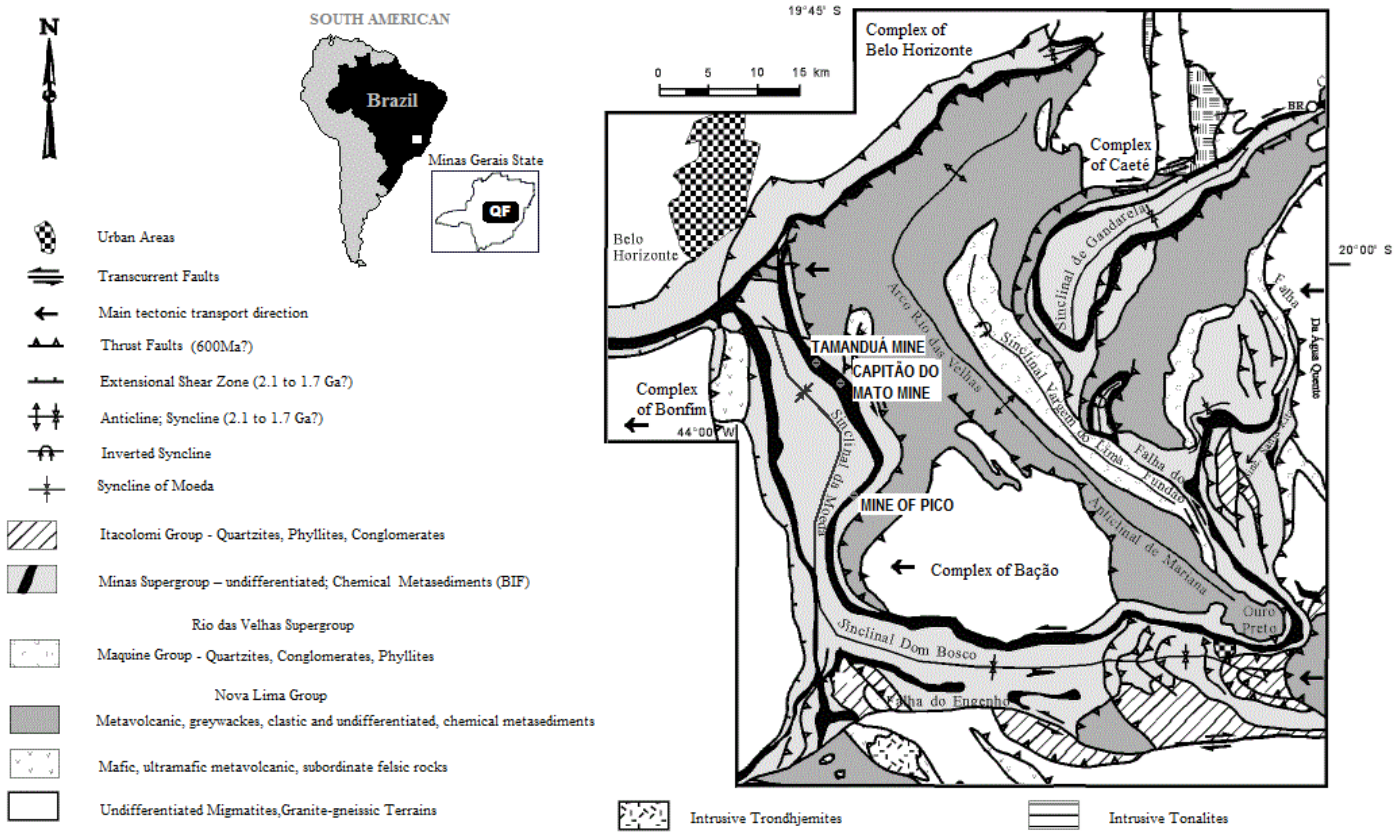

Fig. 1 – Geological Map of the QF Region (modified after Dorr, 1969).

2.1. Geological Characterization

The lithotypes that make up the rock masses of the Tamanduá, Pico and Capitão do Mato mines are composed of the Caraça Group (Moeda and Batatal Formations), Transitional Unit (volcano-sedimentary sequence between the Batatal and the Cauê Formations), Itabira Group (Cauê and Gandarela Formations) and mafic dikes.

The Moeda Formation, at the bottom of this Upper Proterozoic sequence, is composed of quartzites (QZ) of different grain sizes, usually fine to medium, with coarse to microconglomeratic horizons, which compose a fissural aquifer. The Batatal Formation overlies this unit, and is composed of sericitic phyllites (FS), dolomitic phyllites (FD), quartzous and carbonous phyllites and scattered lenses of metachert (MCH). Dolomitic and quartzous phyllites and beds and lenses of metachert make up the Transitional Unit (OPGPM, 2005; Suckau, 2005). This unit underlies itabirites (IB) and hematitic bodies (HM) of the Cauê Formation that is also a good aquifer from which iron ore is extracted in the area covered by the mines (MDGEO 2005 a, b and c). The Batatal phyllite is considered and efficient hydraulic barrier between the aquifers of the Moeda and Cauê Formations (Silva, 2006), notwithstanding the presence of metachert beds and lenses within it and within the transitional unit.

Metric to decametric intrusive mafic dikes (B) derived from gabbros cut the regional structural framework, specially at the Capitão do Mato mine. These dikes act as an efficient hydraulic barrier (OPGPM, 2005).

These geological units' bedding pattern is characterized by steep dip angles, and at the Tamanduá mine, the stratigraphic sequence has been inverted due to intense folding.

2.2. Shear Strength Parameters

From the geological-geomechanical model adopted by the mines company based on the systematic survey of weathering degree data (IPT, 1984) and rock coherence data (Guidicini et al, 1972) and on rock mass classes proposed by Bieniawski (1989), it was possible to compile strength parameters of tested samples from those lithotypes present in the mines; these data were subsequently consolidated (Table 1).

Table 1 – Strength parameters of lithotypes found in the mines.

*Material / Geomechanics Classification**		γ_{nat} / γ_{sat} (kN/m^3)	*Strength Parameters*				*Tests Considered (Unit)*
			Parallel		*Oblique*		
			c' (kN/m²)	*ϕ ' (º)*	*c' (kN/m²)*	*ϕ ' (º)*	
FS (Sericitic Phyllite)	V/VI	18/20			63,3	21	03
	IV	20/22			101,7	32,9	05
	III	23/24			174	38,3	04
	II	28/28			1300	49	01
FD (Dolomitic Phyllite)	VI	18/20			47,8	21,2	08
	V	19/20			52,7	26,1	07
	IV	20/22			116,1	29,4	08
QZ (Quartzite)	VI	20/22			29,4	20,1	05
	V	20/22			29,1	30,5	05
	IV	22/22			40,7	37,5	08
	II/III	24/26			727,5	51,8	03
QX (Micaceous Quartzite)	VI	20/22			29,4	20,1	-
	V	20/22			29,1	30,5	-
	IV	22/22			40,7	37,5	-
	III	24/26			727,5	51,8	-
HM (Hematite)	V/VI	37/40			69	36,8	18
	III/IV	40/44			229,6	40,3	04
	II	45/50			366,7	44	03
IB (Itabirite)	VI/V	25/28	16,6	34,7	51,8	36,6	10 e 12
	III/IV	30/30	31,4	34,1	83,5	40,3	05 e 04
AIF (Argillaceous Itabirite)	V/VI	22/24			83,3	33	03
MCH (Metachert)	V/VI	24/25			56,6	31,7	05
B (Basic Rock)	VI	19/19			36,5	30,9	06

Note: *(After Bieniawski, 1989).

2.3. Hydrodynamic Rock Mass Parameters

The definition of the hydrodynamic properties (hydraulic conductivity and storage) of each material was primarily based on the lithology, with some mapped units being grouped when presenting lithologic similarity among them or when found in minor bodies, considered irrelevant if compared to discretization scale of numerical models.

From hydrogeological numerical models developed for the mines (MDGEO, 2005 a,b,c), the mapped lithologies have been grouped according to their hydrodynamic properties, which resulted in 11 eleven groups (Table 2).

Table 2 – Hydraulic conductivity (*K*), coefficient of specific storage (Ss) and effective porosity (Sy) parameters.

Material	*Kx (m/day)*	*Ky (m/day)*	*Kz (m/day)*	*Ss (m^{-1})*	*Sy*
Itabirite (IB) and medium Hematite (HM)	2.4166	1.1041	1.4166	0.00004	0.0850
Itabirite (IB) and soft Hematite (HM)	1.5000	0.7500	1.0000	0.00004	0.2500
Compact Itabirite (IB)	3.1666	1.4583	1.8333	0.00004	0.0633
Argillaceous Itabirite (AIF)	0.5333	0.4083	0.5333	0.00004	0.0150
Compact Hematite (HM)	3.7500	1.6875	2.2500	0.00006	0.0900
Dolomitic Phyllite (FD)	0.0009	0.0009	0.0009	0.00005	0.0050
Sericitic Phyllite (FS)	0.0010	0.0010	0.0010	0.00005	0.0050
Moeda Quartzite (QZ and QX)	0.1333	0.1366	0.1333	0.00005	0.0203
Basic Intrusive Rock (B)	0.0003	0.0003	0.0003	0.00004	0.0036
Metachert (MCH)	0.1333	0.1333	0.1333	0.00005	0.0100
Covers and breccias	3.0000	3.0000	3.0000	0.00005	0.1000

3. METHODS

The first step was a compilation of geological-geotechnical and hydrogeological characterization data for the pits and an analysis of data provided by VALE.

Based on treatment of these data, we selected three geological-geomechanical sections that represented the typical conditions of the slopes of each mine (Figures 2, 3 and 4), being: sections SE-8750, SE-8850 and SE-9000 – east slope of the Tamanduá Mine; sections SV-8250, SV-8350 and SV-8500 – southeast slope of the Pico Mine; sections SVC-4100, SVC-4300 and SVC-4800 – northeast slope of the Capitão do Mato Mine.

The flow conditions under steady-state conditions of these sections were modeled through the finite elements method, using the SEEP/W® software, using grids with triangular elements . The sections extended to the topographic divide that were assumed to be the same as groundwater divide, therefore, were modeled as an impermeable boundary (zero flow). The downstream and lower boundaries of the sections were located at an average distance of 80 m from the center and between 90 and 100 m of depth in relation to the proposed bottom pit, respectively, also as impermeable boundaries. At the bottom pit level, for each section, we considered that the surface nodes of the grid elements would be assigned zero head due to the condition imposed by the yield of the drawdown wells installed in the iron formation (Cauê Formation). Other slope surfaces were considered to be of the defined flow type, with flow value equivalent to the annual recharge rate within each lithology.

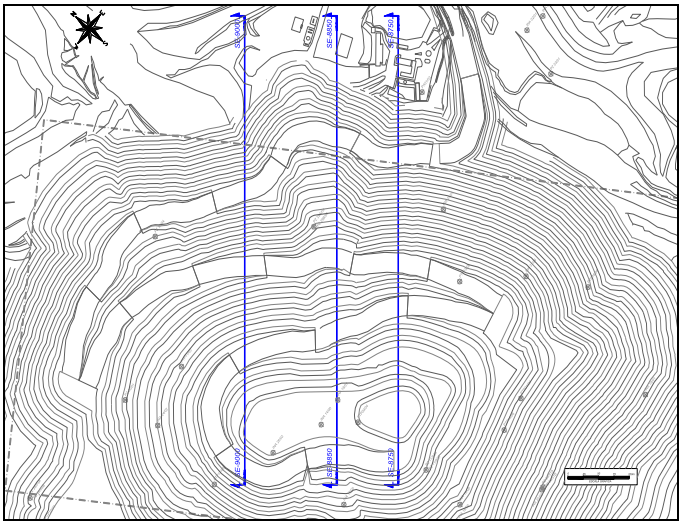

Fig. 2 – Location of sections SE-8750, SE-8850 and SE-9000 – Tamanduá mine pit.

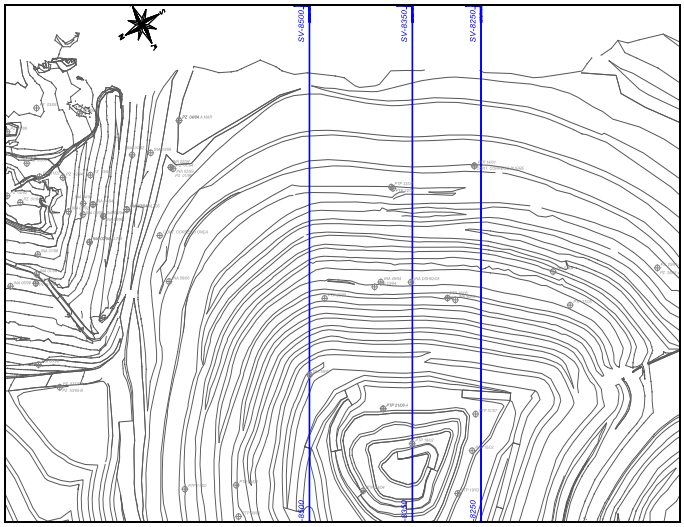

Fig. 3 – Location of sections SV-8250, SV-8350 and SV-8500 – Pico Mine.

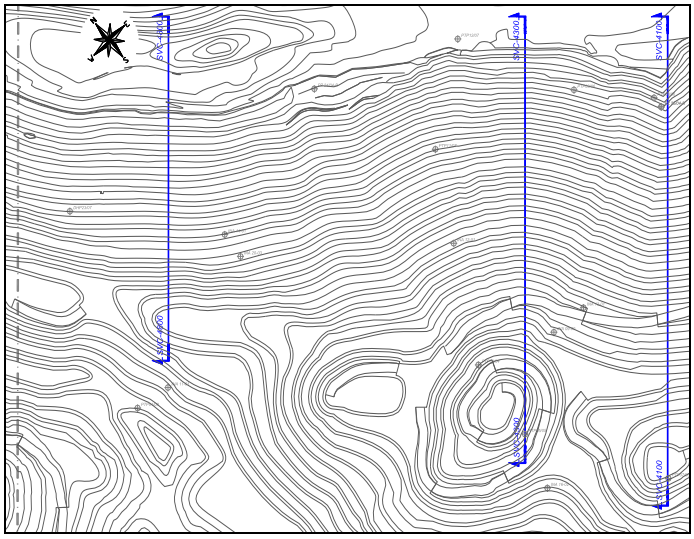

Fig. 4 – Location of sections SVC-4100, SVC-4300 and SVC-4800 - Capitão do Mato Mine.

Based on field data (e.g.: Scarpelli, 1994), we assumed that the occurrence of discontinuities within the lithologies, including the Batatal Formation, is of such a magnitude that they can be treated as a fractured medium of equivalent porosity (Bear & Verruijt, 1987), which allows the application of the finite elements method.

For the purpose of estimating recharge values and pore pressures for each material, we assumed that the hydraulic conductivity of the unsaturated zone varies with suction according to the Fredlund and Xing model (1994). Once established the vertical saturated hydraulic conductivity values (Table 2) of each material, the Fredlund and Xing (1994) method was applied using the available SEEP/W® interface to produce the conductivity variation vs. suction curve (Figure 5).

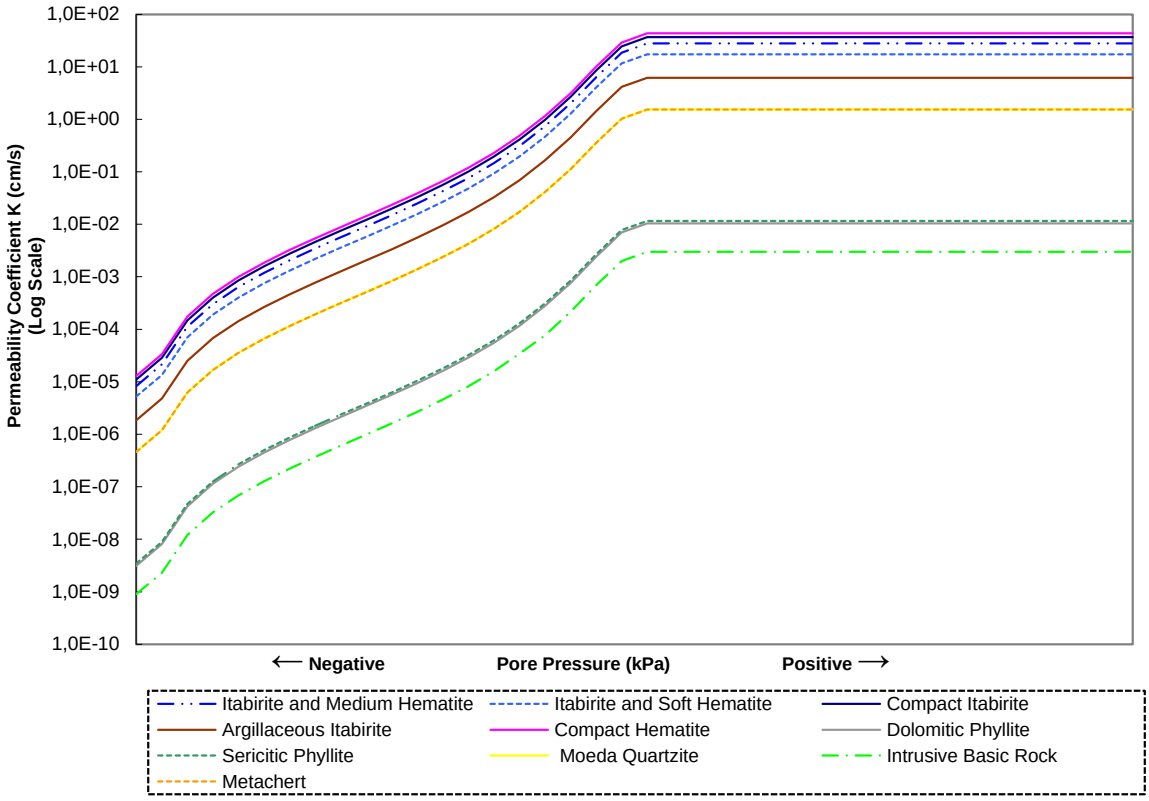

Fig. 5 – Characteristic curves of the lithotypes of the Tamanduá, Pico and Capitão do Mato Mines.

We assumed that the unsaturated-flow zone follows Richards' Equation (Ventura, 2009) and that the hydraulic conductivity values can be calculated through procedures usually employed for unconsolidated materials with intergranular porosity, similarly to the Fredlung & Xing model (1994). Due to the unavailability of information on the actual permo-porosity conditions, we adopted a representative curve for all arenaceous materials using the SEEP/W® databank. This type of approach has been applied to fractured media (Liu et al, 2002), due to the difficulty of employing more sophisticated models and also because we deemed more practical employing it rather than assuming constant conductivity values within the unsaturated zone Therefore, for flow modeling, back-analysis was used to calculate the recharge by varying the flow values within the cells of the upper boundary of the sections, considering the conductivity values of the respective characteristic curves and other boundary conditions already discussed, until the average water-table elevations could be evidenced onsite.

The flow boundary conditions of the upper surface of the slopes, where the Batatal phyllite and the Moeda quartzite prevail, were established from water line (WL) indicators monitoring data presented by Ventura (2009).

The stability analyses were run with the support of the SLOPE/W® software, also incorporating previous results simulated via the SEEP/W® software. Even though the slopes will be implemented in rock masses of different degrees of fracturing and weathering, we assumed that the limit equilibrium methodology would be appropriate for the slope stability studies (Ventura, 2009); this is the usual practice adopted for other nearby mines (Silva, 2006; and Zea Huallanca, 2004).

Stability analyses were developed for six distinct scenarios. For each scenario and each geological section, we assessed the variation of the coefficients of safety on two failure surfaces. The first is the critical surface, automatically generated, which corresponds to the lowest factor of safety. The second was specified as the surface that would involve the greatest number of benches (global failure) and compulsorily intercept the groundwater under the initial calibration condition (scenario 1). This surface was taken into consideration because in some sections of the Pico and Capitão do Mato mines the critical surface does not intercept the WL, an essential condition to enable the analysis of the flow pattern of slope stability.

The stability conditions were analyzed for scenarios 1 to 5 based on the respective flow analyses, employing the strength parameters compiled in Table 1. For scenario 6, we adopted the same conditions of scenario 1, but assumed a constant vertical hydraulic head (vertical flow equipotential lines), as usually done for stability analyses that do not count on previous flow modeling. Therefore, this scenario was the basis for estimating the influence of ascending and descending flow components on slope stability.

4. ANALYSIS OF THE INFLUENCE OF HYDRAULIC BARRIERS

The recharge values produced through back-analysis by varying the flow of cells that compose the upper boundary of the sections are shown in Table 3.

The steady-state flow simulation of each section (2D modeling) involved a five-scenario analysis, seeking to understand the influence of the hydraulic conductivity of the Batatal Formation (FB) on the flow pattern and slope stability conditions. The initial scenario (1) had its flow conditions defined from the consolidated hydrodynamic parameters (Chart 2), and WL calibration according to piezometric monitoring data (Ventura, 2009). The hydraulic conductivity values of the Batatal phyllites (Scenarios 2 and 3) have been reduced 5 and 10-fold, respectively, for scenario 1. For scenarios 3 and 4, the hydraulic conductivity values of the materials have been 5 and 10-fold, respectively.

The magnitude of the hydraulic conductivity variation per scenario was established based on discontinuity data of phyllite rock masses of the Batatal Formation surveyed by Scarpelli (1994). Thus, from this data and the Cubic Law (Snow, 1969), it was possible to estimate potential conductivity variations within these rock masses (sericitic and dolomitic phyllites) due to rock mass discontinuities. The extreme conductivity values employed in the models, specially the higher ones, are quite unrealistic, but have been used to simulate the Batatal Formation effect on flow conditions (Ventura, 2009).

Table 3 – Recharge back-analysis values.

Geotechnical Section		Aquifer Recharge (cm/s)				
		Quartzites (QZ and QX)	**Iron Formation (IB /HM)**	**Metachert (MCH)**	**Dolomitic Phyllites (FD)**	**Sericitic Phyllites (FS)**
Tamanduá Mine	SE - 8750	7.00E-06	5.05E-07	5.05E-07	1.52E-07	1.52E-07
	SE - 8850	3.00E-06	5.05E-07	5.05E-07	1.52E-07	1.52E-07
	SE - 9000	9.00E-07	5.05E-07	5.05E-07	1.52E-07	1.52E-07
Pico Mine	SV - 8250	5.00E-07	5.05E-07	5.05E-07	1.52E-07	1.52E-07
	SV - 8350	6.00E-07	5.05E-07	5.05E-07	1.52E-07	1.52E-07
	SV - 8500	4.50E-07	5.05E-07	5.05E-07	1.52E-07	1.52E-07
C. do Mato Mine	SVC - 4100	-	5.05E-07	5.05E-07	1.52E-07	4.80E-07
	SVC - 4300	-	5.05E-07	5.05E-07	1.52E-07	4.00E-07
	SVC - 4800	5.20E-07	5.05E-07	5.05E-07	1.52E-07	4.00E-07

4.1. Results

The flow conditions defined for sections SE-8850 and SVC-4300 according to some of the scenarios can be seen in Figures 6 and 7, respectively. In each section, arrow length is proportional to flow magnitude.

These sections are characterized by low-permeability horizons (basic rock dike – section SE-8850) and permeable horizons (metachert layer - section SVC-4300) next to the Batatal Formation phyllites.

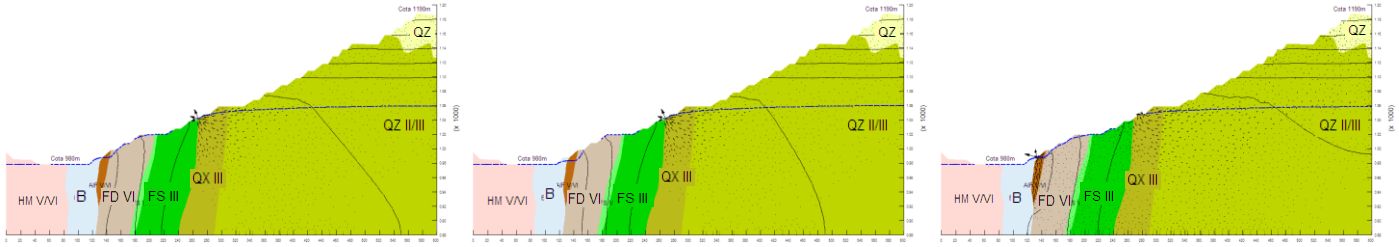

Fig. 6 - Section SE-8850 - Tamanduá Mine – Scenarios 1, 2 and 4, respectively.

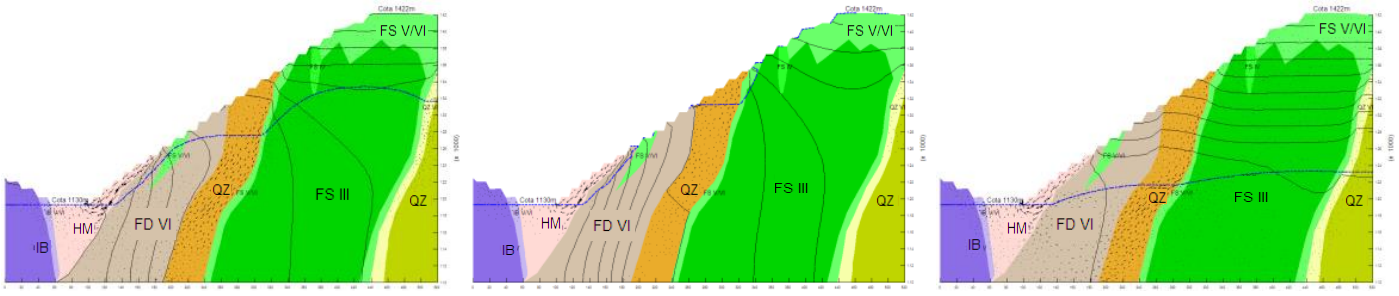

Fig. 7 - Section SVC-4300 - Capitão do Mato Mine – Scenarios 1, 2 and 4, respectively.

Figures 8 and 9 show some examples of stability analysis results.

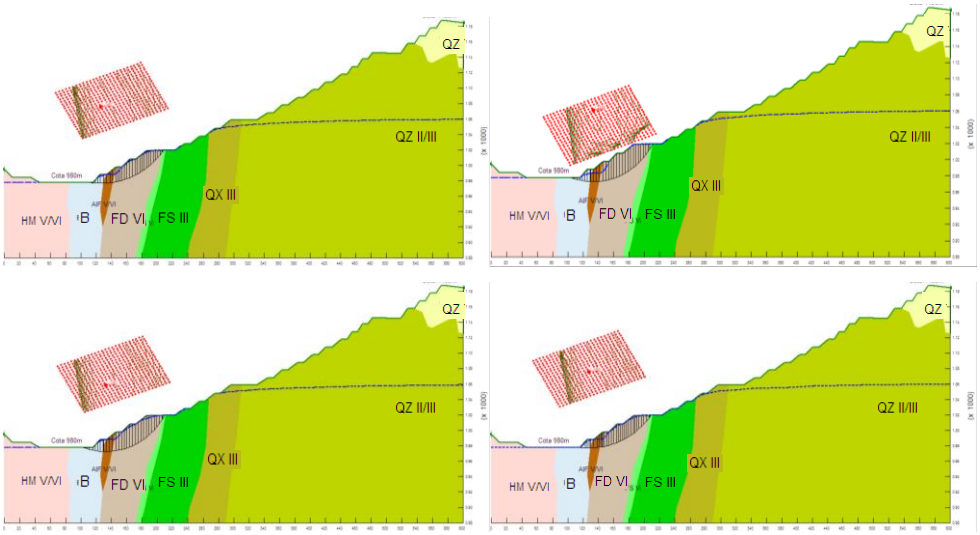

Fig. 8 – Section SE-8850 - Tamanduá Mine – Critical surface, stability analysis of Scenarios 1, 2, 4 and 6, respectively.

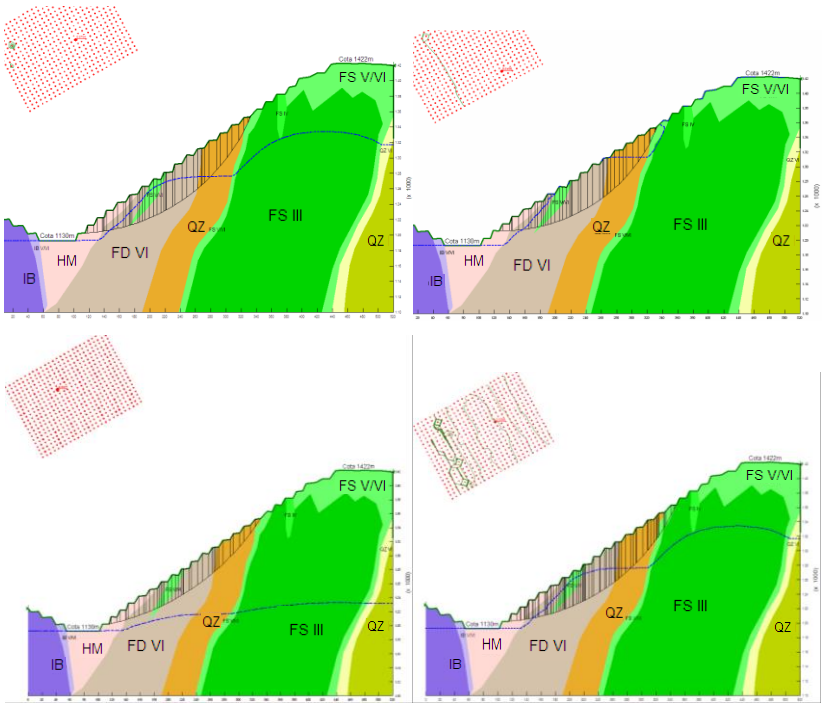

Fig. 9 – Section SVC-4300, Capitão do Mato Mine – Critical surface, stability analysis of Scenarios 1, 2, 4 and 6, respectively.

The factors of safety (F.S.) produced for the six scenarios analyzed for three sections of each mine, considering critical and rock mass failure situations, are shown in Table 4.

Table 4 – Factors of safety per scenario and per section.

Cross Section		Failure Surface	F.S. – Finite Element Method																	
			Scenario 1			Scenario 2			Scenario 3			Scenario 4			Scenario 5			Scenario 6		
			Bishop	Janbu	M. Price	Bishop	Janbu	M. Price	Bishop	Janbu	M. Price	Bishop	Janbu	M. Price	Bishop	Janbu	M. Price	Bishop	Janbu	M. Price
Tamanduá Mine	SE-8750	Crítica	2,198	2,184	2,243	2,038	1,889	1,988	2,030	1,866	1,985	2,247	2,174	2,242	2,231	2,165	2,227	2,244	2,178	2,240
		10651	2,488	2,358	2,509	2,478	2,347	2,499	2,476	2,346	2,500	2,519	2,395	2,540	2,553	2,434	2,574	2,478	2,355	2,499
	SE-8850	Crítica	1,109	1,025	1,141	1,186	1,063	1,229	1,234	1,095	1,281	1,090	0,976	1,136	1,093	0,983	1,134	1,078	0,997	1,109
		7242	1,433	1,400	1,431	1,493	1,451	1,490	1,480	1,444	1,526	1,434	1,401	1,432	1,458	1,428	1,456	1,530	1,507	1,531
	SE-9000	Crítica	0,803	0,681	0,816	0,782	0,658	0,794	0,787	0,649	0,791	1,423	1,233	1,428	1,597	1,453	1,614	0,937	0,804	0,953
		5288	0,965	0,886	0,958	0,943	0,864	0,936	0,939	0,860	0,932	1,756	1,644	1,751	1,790	1,672	1,782	1,125	1,037	1,117
Pico Mine	SV-8250	Crítica	1,352	1,281	1,344	0,916	0,820	0,929	0,890	0,791	0,905	1,344	1,281	1,352	1,342	1,278	1,349	1,343	1,280	1,350
		8106	1,444	1,294	1,418	1,087	0,960	1,118	1,112	0,970	1,150	1,435	1,309	1,459	1,435	1,309	1,459	1,417	1,293	1,443
	SV-8350	Crítica	1,291	1,225	1,281	1,000	0,813	0,997	0,833	0,775	0,846	1,281	1,225	1,291	1,281	1,225	1,291	1,274	1,236	1,282
		6832	1,607	1,398	1,579	1,276	1,072	1,320	1,256	1,053	1,301	1,579	1,398	1,608	1,579	1,398	1,608	1,579	1,398	1,601
	SV-8500	Crítica	1,101	1,038	1,057	0,671	0,620	0,684	0,648	0,599	0,662	1,094	1,038	1,101	1,094	1,038	1,101	1,094	1,025	1,100
		2613	1,164	1,051	1,156	0,730	0,643	0,753	0,713	0,628	0,736	1,164	1,063	1,171	1,167	1,060	1,175	1,155	1,052	1,164
Capitão do Mato Mine	SVC-4100	Crítica	0,856	0,787	0,847	0,349	0,329	0,357	0,253	0,247	0,258	0,933	0,889	0,941	0,928	0,887	0,937	0,846	0,786	0,855
		1936	0,898	0,815	0,899	0,882	0,803	0,868	0,789	0,719	0,777	1,071	0,962	1,060	1,074	0,964	1,063	0,899	0,816	0,899
	SVC-4300	Crítica	0,870	0,817	0,872	0,649	0,599	0,650	0,647	0,597	0,648	0,996	0,957	0,993	1,002	0,961	0,998	0,863	0,816	0,860
		3930	0,989	0,949	1,001	0,732	0,679	0,725	0,730	0,677	0,723	1,240	1,154	1,216	1,256	1,166	1,231	1,001	0,946	0,988
	SVC-4800	Crítica	1,084	1,039	1,068	0,726	0,687	0,742	0,666	0,637	0,682	1,068	1,039	1,084	1,071	1,041	1,086	1,102	1,063	1,121
		1587	1,258	1,179	1,250	0,830	0,755	0,838	0,808	0,731	0,817	1,270	1,196	1,277	1,270	1,196	1,277	1,243	1,172	1,251

4.2. Discussion of Results

Generally speaking, the WL of all sections behaved in a coherent manner, following the hydraulic conductivity of quartzites and metacherts (high) and phyllites (low), and the hydraulic gradient of these materials (low and high, respectively) (Figure 7). We also verified that the metachert layers play an important drainage role within the Batatal Formation phyllites.

For major slopes, the location and thickness of the hydraulic barriers strongly control the degree of saturation of slope surfaces. For situations when a thicker barrier stands sub-vertically and outcrops on the more elevated slope portions, it is highly likely that the intermediate and, preferably, the lower portion are strongly saturated. Other high-saturation situation can occur when thick hydraulic barrier levels prevent the upstream WL from being affected by the drawdown operations carried out on the pit bottom surface.

The flow and F.S. values behave differently in the three mines, especially when the geological-geotechnical characteristics of the materials and the geometry of the pit slopes are taken into consideration. The deeper failure surfaces with lower F.S. could be found in the Capitão do Mato mine, whose overall slope angle is the steepest of them all. The F.S. calculated for the ultimate pit situation was, sometimes, lower than 1,0, pointing out to the need of adopting control measures so that future stability could be ensured.

If the results of the three limit equilibrium methods are compared, the F.S. values produced by the Janbu method are lower (Chart 5), i.e., more conservative. The results of the Bishop and Morgenstern Price methods are similar, but traditionally, the latter is considered more accurate. This similarity is explained by the fact that for circular failures, the forces among slices are not contemplated by the Morgenstern Price method.

Table 5 – Comparison of average F.S. values – Limit Equilibrium method.

Bishop is higher		Janbu is higher		M. Price is higher	
Janbu	M. Price	Bishop	M. Price	Bishop	Janbu
7.46%	- 0.65%	- 8.24%	- 8.97%	0.63%	8.03%

The variation imposed on the hydraulic conductivity of dolomitic phyllites (FD) and sericitic phyllites (FS) of the Batatal Formation provided different conditions of groundwater flow and WL configuration, which, consequently, result in alterations of geometric features and location of critical failure surfaces. For example, critical failure surfaces tend to be shallower in drained rock masses (e.g., scenario 5, Figure 7) and deeper in saturated rock masses (e.g., scenario 3, Figure 7).

The existence of more permeable units within the Batatal phyllite layers, such as metachert (MCH), results in a positive safety effect because they pull the WL down (e.g., scenario 1, Figure 8). However, less permeable units, such as basic dikes (B), lead to opposite conditions, and tend to create upstream ascending flows. This phenomenon can be clearly observed in section SE-8850 (Figure 6) of the Tamanduá mine, where the F.S. is the mine's lowest (Chart 4).

F.S. variation (Chart 4) confirms the general trend predicted, i.e., the lower the hydraulic conductivity values of phyllites (scenarios 2 and 3) the higher the phreatic levels, with consequent reduction of seepage flowing through phyllites and F.S. values. The rise of the phreatic surface allows some unsaturated phyllite sectors to become saturated, leading to lower effective stresses. Other relevant aspect associated with lower F.S. values was an increase of ascending flows within quartzites from the Moeda Formation located downstream the phyllites, thus reducing shear stress values. This affirmative can be proved due to the fact that critical failures developed for some sections of scenarios 1, 4 and 5 are located in the first benches at the toe of the slope, and can be considered shallow failures, in opposition to those developed for scenarios 2 and 3 (higher degree of saturation of phyllites), which became deeper and located in intermediate benches (immediately upstream the phyllites), and submitted to ascending flows.

When the hydraulic conductivity of phyllites was increased (scenarios 4 and 5), seepage through the phyllites tended to increase as the WL was drawn down with consequent increase of F.S. values. This behavior could also be explained by the diminished presence or inexistence of ascending flows (e.g., Figure 7). Section SE-8850 of the Tamandua Mine is the only exception as a result of the presence of a diabase dike (B) at the toe of the slope (Figure 6). However, in a general way, it is worth emphasizing that the results of these scenarios showed phreatic surface configurations incompatible with the field reality, but that are presented herein for trend analysis.

Thus, the WL position is quite influenced by the hydraulic conductivity of the Batatal Phyllite (FS and FD). When it is reduced five fold (scenario 2) or increased five fold (scenario 4), the WL position is strongly altered. However, WL and FS values varied less between scenarios 2 and 3 and also between scenarios 4 and 5.

The F.S. values of section SE-8850 of the Tamanduá Mine (Chart 4) show the same trend between the scenarios. But this section has a distinctive feature that is the presence of a diabase dike (B) outcropping on the pit bottom surface and on the first slope bench, which allows atypical groundwater flow conditions. The critical failure surfaces of all six scenarios analyzed are shaped the same and mobilize the first inter-ramp slope that has three benches composed of dolomitic phyllites and one bench composed of argillaceous itabirites, which contacts the dike. The F.S.'s relative to the critical surfaces of scenarios 2 and 3 (Chart 4) are higher due to the reduced groundwater flow that ascends through argillaceous itabirites between the dolomitic phyllite layer and the dike. The thin layer of argillaceous itabirite (AIF) sustains saturation conditions lower than those of other scenarios. Under situations that the phyllite layers are more permeable, scenarios 4 and 5, allowing an increased seepage flow through them, it is likely that ascending flow conditions are created within the argillaceous itabirite due to the barrier imposed by the dike (scenario 4, Figure 6), within which, under ascending flow conditions, the effective stress tends to be lower with consequent F.S. reduction.

The scenario 6 analyses, considering horizontal flow conditions, (vertical equipotential lines), showed F.S. values similar to those of scenario 1. However, under situations of high vertical flow components, The F.S. values of scenario 6 tend to vary significantly if compared to those of that scenario. This issue is directly related to the vertical flow components ignored in scenario 6. If pit bottom surfaces are not considered for being less susceptible to rock slides due to the ultimate pit rock masses of higher strength found therein (Cauê Formation), ascending flows could only be identified (scenario 1) in the Tamanduá mine slopes located immediately upstream the sericitic phyllite of the Batatal formation. The higher F.S. value (scenario 6) calculated for the mine sections is explained by the fact that the ascending flows were not taken into account, which led to F.S. overestimation. In cases when the value adopted for the hydraulic conductivity of the Batatal phyllite was lower (scenarios 2 and 3), this problem was even more serious, because negative pressures were more significant. For these cases, the usual practice adopted for limit equilibrium stability analyses of considering the hydraulic potential constant on a vertical plane may lead to F.S. underestimation.

As prognosticated by the theory, hydraulic conductivity variations at lithologic contacts lead to refraction of flow lines (e.g., scenario 4, Figure 7). These minor refractions can induce, locally, flows with ascending components and trigger minor mass displacements, not analyzed herein.

Depending on the special arrangement of the less permeable geological layers, localized ascending flow situations may develop, with consequent reduction of effective stresses (seepage force) and of the slope F.S. values. Minor variations of the hydraulic conductivity of the phyllitic rock mass may result in higher WL, with consequent reduction of the slope F.S. values.

Sub-vertical unsaturated flows may lead to a less intense effect of the apparent cohesion within rock masses of low geomechanical quality. However, the numerical routine of the SLOPE/W® software does not take such influence into consideration. As the saturation rises, the rock mass unit weight also rises. These processes may reduce the safety conditions and result in slope failure. Usually, in rock masses of higher degree of saturation

the critical failure surface becomes deeper than other surfaces developed for drained rock masses.

4.3. Conclusions

This study comprehended a parametric analysis of the probable influence of less permeable units of the Batatal Formation on the flow and stability conditions. Thus, the study findings were:

- The analysis of the stability condition together with the results of the seepage analysis was adequate to achieve the objective proposed;
- The use of indirectly-estimated hydraulic conductivity curves is the preferred option, rather than assuming the recharge as being evenly distributed among all geological units;
- Slope F.S. values depend strongly on the hydraulic conductivity (HC) of the Batatal phyllite, given that minor HC variations led to significant F.S. variations;
- The vertical ascending flow components are relevant for the safety of the slopes and may trigger local failures. Major failures are less affected by such components, at least for the conditions assumed herein, except for section SE-8850 of the Tamanduá mine, which undergoes an atypical situation represented by a basic rock dike;
- Likewise, vertical descending flow components, such as those induced by strongly conductive layers, e.g., metacherts, tend to draw the phreatic surface down and significantly increase the F.S.;
- The groundwater flow follows some basic geotechnical principles, seeping through the route on which energy is spent the least. Therefore, it concentrates along segments of narrower layers and reduced permeability, as verified in the analyses developed;
- Under situations of high hydraulic head upstream low-conductivity layers, high hydraulic gradients develop inside these layers and, occasionally, water springing may also occur at the contact between them;
- As the saturation condition increases, the unit weight also increases, with consequent reduction of the safety conditions for most cases, thus influencing the location and the geometric characteristic of the critical failure. Rock masses of higher degree of saturation, steeper slope angle and lower strength parameters, the critical failure surface becomes deeper.

5. ACKNOWLEDGMENT

The authors thank VALE for providing data and information used in the study of the Tamanduá, Pico and Capitão do Mato mines.

REFERENCES

1. Patton, F.D. and Hendron Junior, A.J. 1974. General report on Mass Movements. In *Int. Congress of the IAEG*. 2nd, 1974, São Paulo. Proc… São Paulo: ABGE. v.2, p. 1-57.
2. Freeze, R.A. and Cherry, J.A. 1979. *Groundwater*. New Jersey: Prentice – Hall. 604 p.
3. Bishop, A. W. 1955. The Use of the Slip Circle in the Stability Analysis of Slopes. *Géotéchnique*, vol. 5, p. 7-17.
4. Janbu, N. 1968. *Slope Stability Computations. Soil Mechanics and Foundation Engineering Report*. Technical University of Norway, Tronheim.
5. Morgestern, N.R. and Price, V.E. 1965. The Analysis of the Stability of General Slip Surfaces. *Geotechnique*, vol. 15, PP. 79-93.
6. Dorr, J.V.N. 1969. Physiographic, Stratigraphic and Structural Development of the Quadrilátero Ferrífero, Brazil. U. S. Geol. Survey, Washington. 110p.
7. Alkmin, F.F. and Marshak, S. 1998. Transamazonian orogeny in the Southern São Francisco Craton region, Minas Gerais, Brazil: evidence for Paleoproterozoic collision and collapse in the Quadrilátero Ferrífero. Precambrian Research, 29-58.
8. OPGPM 2005. Geologia Estrutural da Mina Capitão do Mato – MBR. Ouro Preto Geologia e Pesquisa Mineral Ltda. Nova Lima-MG, 2-28.
9. Suckau, V. 2005. Relatório de reavaliação de reservas das minas Tamanduá e Capitão do Mato. Relatório para o DNPM.
10. MDGEO 2005a. Relatório do modelo numérico do fluxo d'água subterrânea da Mina do Tamanduá. REL_MBR_TAM_05_05. Belo Horizonte: MBR, v.1.
11. MDGEO 2005b. Relatório do modelo numérico do fluxo d'água subterrânea da Mina Capitão do Mato. REL_MBR_CMT_01_05. Belo Horizonte: MBR, v.6.
12. MDGEO 2005c. Relatório do modelo numérico do fluxo d'água subterrânea da Mina do Pico. REL_MBR_PIC_011_05. Belo Horizonte: MBR, v.1.
13. Silva, E.M. 2006. *Análise de estabilidade de taludes em solos de alteração de rochas metamórficas do quadrilátero ferrífero*. Dissertação de Mestrado. Viçosa-MG, UFV. p. 38-87.
14. IPT 1984. Estudos Geológico-geotécnicos para caracterização e classificação de maciços rochosos para projetos de engenharia (túneis, lavra a céu aberto, e barragens). *Instituto de Pesquisas Tecnológicas*. São Paulo. (IPT – Relatório, 19569).
15. Guidicini, G., Nieble, C.M., Cordnides, A.T., Berrino, S.E. and Rodrigues, J.D. 1972. Um método de classificação geotécnica preliminar de maciços rochosos. In: *Semana Paulista de Geologia Aplicada*, 4, São Paulo. Anais... São Paulo: ABGE, v. 3, p. 285-331.

16. Bieniawski, Z.T. 1989. *Engineering rock mass classification.* New York: John Wiley. V. 15, p. 335-344.

17. Scarpelli, A.G. 1994. *Classificação Geomecânica Aplicada a Avaliação da Estabilidade de Taludes em Minas de Ferro do Quadrilátero Ferrífero*. Dissertação de Mestrado. São Carlos-SP, USP, 187 p.

18. Bear, J. and Verruijt, A. 1987. *Modeling Groundwater Flow and Pollution*. D.Reidel Publishing Company, 1987, 413p.

19. Fredlund, D.G. and Xing, A. 1994. Equations for the soil-water characteristic curve. *Canadian Geotechnical Journal*, 31 (3): 521-32.

20. Ventura, L.C. 2009. *Análise da influência de barreiras hidráulicas no padrão do fluxo e na estabilidade de taludes de cavas a céu aberto de minas de ferro do Quadrilátero Ferrífero, MG*. Dissertação de Mestrado. Núcleo de Geotecnia, Escola de Minas, UFOP. Ouro Preto, pp. 10-221.

21. Liu, H.H., Bodvarsson, G.S. and Hudson, D. 2002. *Large-scale Constitutive Relationships for Unsaturated Flow in Fractured Rocks*. Lawrence Berkeley National Laboratory Berkeley, CA and U.S. Geological Survey Sacramento, CA. 11 p.

22. Zea Huallanca, R.H. 2004. *Mecanismo de ruptura em taludes altos de mineração a céu aberto*. Dissertação de Mestrado. São Carlos, USP, p. 3-32.

23. Snow, D.T. 1969. *Anisotropic permeability of fractured media*. Water Resources Research 5(6), 1273–1289.